Available online at www.sciencedirect.com
SCIENCE DIRECT®
Journal of Organometallic Chemistry 689 (2004) 791–800
Journal of Organometallic Chemistry
www.elsevier.com/locate/jorganchem

Unusual chemical reactivity in the reactions of $Re_2(CO)_8(\mu\text{-}H)(\mu\text{-}\eta^1,\eta^2\text{-}CH{=}CHBu)$ with 2,3-bis(diphenylphosphino)maleic anhydride (bma) and $Re_2(CO)_8$(bma) with $Ni(cod)_2$: X-ray diffraction structures of $Re_2(CO)_8$(bma), zwitterionic $Re(CO)_4[Re(CO)_4(bma)]$, and the phosphido-bridged complex $Re_2(CO)_8[\mu\text{-}\eta^1,\eta^1\text{-}\overline{C{=}C(PPh_2)C(O)OC(O)}](\mu\text{-}PPh_2)$

Simon G. Bott [a,*], Kaiyuan Yang [b], Michael G. Richmond [b,*]

[a] Department of Chemistry, University of Houston, Houston, TX 77204, USA
[b] Department of Chemistry, University of North Texas, Denton, TX 76203, USA

Received 9 July 2002; accepted 22 October 2003

Abstract

The reaction between $Re_2(CO)_8(\mu\text{-}H)(\nu\text{-}\eta^1,\eta^2\text{-}CH{=}CHBu)$ (**1**) and the diphosphine ligand 2,3-bis(diphenylphosphino)maleic anhydride (bma) proceeds slowly at room temperature to furnish the expected dirhenium compound $Re_2(CO)_8$(bma) (**2**) and the zwitterionic compound $Re(CO)_4[Re(CO)_4(bma)]$ (**3**). Both **2** and **3** have been isolated and characterized in solution by IR and ^{31}P NMR spectroscopy, in addition to X-ray crystallography. The solid-state structure of **2** reveals a bridging bma ligand that spans the Re–Re vector and whose $Re(CO)_4$ moieties exhibit a staggered rotational geometry. **3** consists of a $Re(CO)_4$ unit that is coordinated to the bma ligand in a chelating fashion by the two PPh_2 moieties, with the other $Re(CO)_4$ unit being π-bound to the alkene bond of the bma ligand. Thermolysis of $Re_2(CO)_8$(bma) in the presence of added $Ni(cod)_2$ affords the phosphido-bridged complex $Re_2(CO)_8[\mu\text{-}\eta^1,\eta^1\text{-}\overline{C{=}C(PPh_2)C(O)OC(O)}](\mu\text{-}PPh_2)$ (**4**), whose identity has been established by solution spectroscopic methods and X-ray diffraction analysis. The redox properties of $Re_2(CO)_8$(bma) have been examined in detailed by cyclic voltammetry and constant-potential coulometry, where two fully reversible, one-electron reductions ($0/1^-$ and $1^-/2^-$) were observed at $E_{1/2} = -0.38$ V and $E_{1/2} = -1.29$ V in CH_2Cl_2. The reduction behavior is discussed relative to the nature of the LUMO level, which has been determined by extended Hückel MO calculations. The redox chemistry and the LUMO in $Re_2(CO)_8$(bma) are contrasted with the known redox chemistry and the LUMO composition of the mononuclear species $BrRe(CO)_3$(bma) and related bma-substituted complexes. The MO calculations on $Re(CO)_4[Re(CO)_4(bma)]$ (**3**) reveal that the HOMO and LUMO levels are formed from the HOMO of the d_8-ML_4 fragment $Re(CO)_4^-$ and its interaction with the $\psi_4\pi^*$ antibonding MO of the bma ligand on the $[Re(CO)_4(bma)]^+$ fragment.

Keywords: Dirhenium compounds; Diphosphine ligand; Redox chemistry; Extended Hückel MO calculations

1. Introduction

The diverse coordination chemistry and reactivity exhibited by the diphosphine ligand 2,3-bis(diphenylphosphino)maleic anhydride (bma) and its close relative 4,5-bis(diphenylphosphino)-4-cyclopenten-1,3-dione (bpcd) have been duly demonstrated in recent years [1]. The utility of bma- and bpcd-substituted complexes to serve as electron reservoirs in chemical and electrochemical reduction sequences and the ability of the corresponding $18 + \delta$ complexes to modulate dissociative CO loss in sundry metal-carbonyl compounds

* Corresponding authors. Tel.: +1-713-743-2771 (S.G. Bott), +1-940-565-3548 (M.G. Richmond).
E-mail addresses: sbott@uh.edu (S.G. Bott), cobalt@unt.edu (M.G. Richmond).

0022-328X/$ - see front matter © 2003 Published by Elsevier B.V.
doi:10.1016/j.jorganchem.2003.10.043

have been thoroughly explored [2]. One of our main interests in this genre of diphosphine ligand derives from our initial observation of facile P–C bond cleavage that often accompanies the attachment of these ligands to polynuclear metal clusters, as depicted in Eq. (1) for the tricobalt cluster $PhCCo_3(CO)_7$(bma) [3]. Besides the facile activation of this ligand at a wide variety of polynuclear clusters by both C(maleic anhydride)–P and Ph–P manifolds [4], we have also observed that this particular ligand is capable of ambulatory migration about a cluster polyhedron via discernable bridging and chelating phosphine isomers. The dynamic isomerism exhibited by the bma ligand, in the documented paradigms to date, proceeds by an intramolecular path that does not require CO loss.

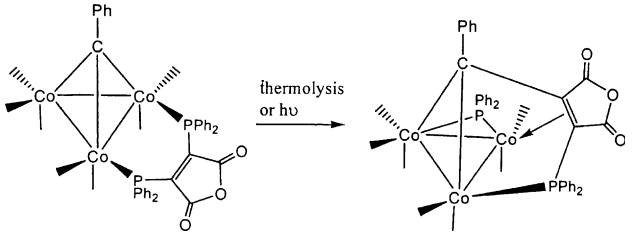

(1)

Several years ago we published our results on the synthesis and redox investigation of the rhenium complexes *fac*-$BrRe(CO)_3(bma)^{0/1-}$. Here the effects of electron accession in going from the neutral starting material to the reduced $18+\delta$ complex, *fac*-$BrRe(CO)_3(bma)^{1-}$, were fully analyzed by IR spectroscopy, X-ray crystallography, and MO calculations [5]. Given the dearth of structurally characterized rhenium complexes that contain an ancillary bma ligand, we have embarked on the synthesis and study of other such rhenium complexes [6]. Herein we present our data on the reaction between the activated hexeny compound $Re_2(CO)_8(\mu\text{-}H)(\mu\text{-}\eta^1,\eta^2\text{-}CH{=}CHBu)$ and bma, which affords $Re_2(CO)_8$(bma) (**2**) and $Re(CO)_4[Re(CO)_4(bma)]$ (**3**). The cleavage of the P–C bond in **2** by added $Ni(cod)_2$ gives the corresponding phosphido-bridged dirhenium compound $Re_2(CO)_8[\mu\text{-}\eta^1,\eta^1\text{-}C{=}C(PPh_2)C(O)OC(O)](\mu\text{-}PPh_2)$ (**4**). Compounds **2**–**4** have been fully characterized in solution and their molecular structures established by X-ray crystallography.

2. Experimental

2.1. General methods

The bma ligand used in these studies was synthesized from 2,3-dichloromaleic anhydride (Aldrich Chemical Co.) and Ph_2PTMS according to the known procedure [7]. The latter chemical was prepared from Ph_2PH and TMSCl [8], while the $Re_2(CO)_{10}$ was prepared from $NaReO_4$ and CO, employing the carbonylation procedure of Heinekey [9]. The hexenyl compound $Re_2(CO)_8(\mu\text{-}H)(\mu\text{-}\eta^1,\eta^2\text{-}CH{=}CHBu)$ (**1**) was obtained from the photochemical reaction of $Re_2(CO)_{10}$ and 1-hexene, as originally described by Brown [10]. Cp_2Co was prepared according the procedure of King [11]. The 1-hexene required for the synthesis of compound **1** was passed across a column of activated alumina immediately before its use. All reaction, NMR, and electrochemistry solvents were distilled under argon from a suitable drying agent and stored in Schlenk storage vessels [12]. The tetra-*n*-butylammonium perchlorate electrolyte (TBAP) was purchased from Johnson Matthey Electronics and recrystallized from ethyl acetate/hexane (1:1), followed by drying for at least 48 h under high vacuum. All C and H analyses were performed by Altantic Microlab, Norcross, GA.

The reported infrared data were recorded on a Nicolet 20 SXB FT-IR spectrometer in 0.1 mm NaCl cells, using PC control and OMNIC software, while the ^{31}P NMR spectra were recorded at 121 MHz on a Varian 300-VXR spectrometer. The reported ^{31}P chemical shifts are referenced to external H_3PO_4 (85%), taken to have $\delta = 0.0$. Here positive chemical shifts are to low field of the external standard.

2.2. Synthesis of $Re_2(CO)_8$(bma) and $Re(CO)_4[Re(CO)_4(bma)]$

To 2.00 g (3.07 mmol) of $Re_2(CO)_{10}$ in an Ace Glass photochemical reactor under argon flush was added ca. 250 ml of 1-hexene. The solution was irradiated at 254 nm until the conversion to $Re_2(CO)_8(\mu\text{-}H)(\mu\text{-}\eta^1,\eta^2\text{-}CH{=}CHBu)$ was judged to be complete by IR spectroscopy (ca. 2 h), after which time the solution was transferred to a large Schlenk flask and the 1-hexene was removed under vacuum. At this point, 200 ml of CH_2Cl_2 was added, followed by 1.50 g (3.22 mmol) of bma. The reaction was protected from room light and stirred for at least two weeks, during which time the solution acquired a red color. The progress of the reaction was assessed by periodically monitoring the solution by TLC and IR analyses. Upon the consumption of the starting rhenium compound (>95%), the CH_2Cl_2 solvent was removed and the crude material was extracted with petroleum ether until the remaining residue was pale yellow in color. Since compounds **2** and **3** exhibit substantial decomposition during chromatographic separation over silica gel at room temperature (vide supra), the desired products were isolated in pure form by low-temperature (−78 °C) column chromatography. $Re_2(CO)_8$(bma) was obtained from the column using CH_2Cl_2 as the eluent, followed by $Re(CO)_4[Re(CO)_4(bma)]$ when the eluent was changed to CH_2Cl_2/acetone (9:1). Single crystals of **2** and **3** suitable for combustion analysis and X-ray diffraction examination

were grown from CH_2Cl_2 solutions containing these compounds that had been layered with hexane. Yield of yellow **2**: 0.65 g (19.9%). IR (CH_2Cl_2): ν(CO) 2076 (s), 2025 (s), 1985 (vs), 1959 (m), 1926 (s), 1828 (vw, antisymm anhydride carbonyl), 1775 (s, symm anhydride carbonyl) cm^{-1}. ^{31}P NMR (CH_2Cl_2): δ – 9.37. Anal. Calc. (found) for $C_{36}H_{20}O_{11}P_2Re_2$: C, 40.68 (40.56); H, 1.90 (1.89). Yield of colorless **3**: 0.80 g (24.5%). IR (CH_2Cl_2): ν(CO) 2108 (m), 2080 (m), 2014 (vs), 1996 (vs), 1962 (vs), 1948 (vs), 1781 (w, antisymm anhydride carbonyl), 1723 (m, symm anhydride carbonyl) cm^{-1}. ^{31}P NMR (CH_2Cl_2): δ 39.07. Anal. Calc. (found) for $C_{36}H_{20}O_{11}P_2Re_2$: C, 40.68 (40.56); H, 1.90 (1.95).

2.3. Synthesis of $Re_2(CO)_8[\mu\text{-}\eta^1,\eta^1\text{-}\overline{C{=}C(PPh_2)C(O)OC(O)}](\mu\text{-}PPh_2)$

To 0.20 g (0.19 mmol) of $Re_2(CO)_8$(bma) in 35 ml of toluene was added 0.05 g (0.18 mmol) of $Ni(cod)_2$. The reaction solution was heated at 60–70 °C for less than 1.0 h, followed by TLC analysis in CH_2Cl_2/petroleum ether (1:1), which revealed the presence of a yellow spot ($R_f = 0.47$) and much material that remained at the origin. The material at the origin showed no propensity for migration using a wide variety of developing solvents. The yellow band was isolated by chromatography over silica gel using CH_2Cl_2/petroleum ether (1:1) as the eluent. Single crystals of **4** suitable for combustion analysis and X-ray diffraction examination were grown from CH_2Cl_2 solutions containing **4** that had been layered with hexane. Yield of **4**: 30.0 mg (15.0%). IR (CH_2Cl_2): ν(CO) 2103 (w), 2088 (m), 2039 (m), 2007 (vs), 1976 (vs), 1807 (vw, antisymm anhydride carbonyl), 1743 (m, symm anhydride carbonyl) cm^{-1}. ^{31}P NMR (CH_2Cl_2): δ 100.01 ($J_{P-P} = 19.7$ Hz), 10.50 ($J_{P-P} = 19.7$ Hz). Anal. Calc. (found) for $C_{36}H_{20}O_{11}P_2Re_2$: C, 40.68 (40.54); H, 1.90 (1.97).

2.4. X-ray diffraction structures of compounds 2–4

Selected crystals of **2**–**4** suitable for X-ray diffraction analysis were grown as described above and were each sealed inside a Lindemann capillary, followed by mounting on an Enraf–Nonius CAD-4 diffractometer. After the cell constants were obtained for all three samples, intensity data in the range of $2° \leqslant 2\theta \leqslant 44°$ were collected at 298 K and were corrected for Lorentz, polarization, and absorption (DIFABS). All structures were solved by using standard Patterson techniques, which revealed the positions of the rhenium and phosphorus atoms. In the case of **2**, all non-hydrogen atoms were located with difference Fourier maps and full-matrix least-squares refinement and were refined anisotropically with the exception of the phenyl carbon atoms and the oxygen atoms associated with carbonyl groups. All non-hydrogen atoms in **3** were refined anisotropically with the exception of the ancillary phenyl carbons and some of the carbon atoms belonging to the carbonyl groups and the maleic anhydride moiety. The asymmetric unit of **4** contains half a molecule of hexane that resides on an inversion center. Refinement of compound **4** followed similar data reduction procedures, with all non-hydrogen atoms except for the phenyl and solvent carbon atoms being refined anisotropically. Refinement on **2** converged at $R = 0.0461$ and $R_w = 0.0500$ for 3382 unique reflections with $I > 3\sigma(I)$, while for **3** refinement converged at $R = 0.0439$ and $R_w = 0.0529$ for 2541 unique reflections with $I > 3\sigma(I)$. The refinement for **4** converged at $R = 0.0345$ and $R_w = 0.0381$ for 3163 unique reflections with $I > 3\sigma(I)$.

2.5. Extended Hückel MO calculations

The extended Hückel calculations on $Re_2(CO)_8$(bma), $Re(CO)_4[Re(CO)_4(bma)]$, and $Re_2(CO)_8[\mu\text{-}\eta^1,\eta^1\text{-}\overline{C{=}C(PPh_2)C(O)OC(O)}](\mu\text{-}PPh_2)$ were conducted with the original program developed by Hoffmann [13], as modified by Mealli and Proserpio [14], using weighted H'*ij*s. The input *Z*-matrix for the model compounds $Re_2(CO)_8(H_4\text{-bma})$, $Re(CO)_4[Re(CO)_4(H_4\text{-bma})]$, and $Re_2(CO)_8[\mu\text{-}\eta^1,\eta^1\text{-}\overline{C{=}C(PH_2)C(O)OC(O)}](\mu\text{-}PH_2)$ was constructed from the X-ray fractional coordinates of each compound. Here the phenyl groups were replaced by hydrogens in order to simplify the calculations, with the P–H bond lengths assigned a value of 1.42 Å [15].

2.6. Cyclic voltammetry data

The electrochemical data (CV and CPC) were recorded on a PAR Model 273 potentiostat/galvanostat, equipped with positive feedback circuitry to compensate for *i*R drop. The airtight CV cell used was based on a three-electrode design, and a platinum disk was employed as the working and auxiliary electrodes. The reference electrode utilized a silver wire as a quasi-reference electrode, and the reported potential data are referenced to the formal potential of the Cp_2Fe/Cp_2Fe^+ (internally added) redox couple, taken to have $E_{1/2} = 0.307$ V [16].

3. Results and discussion

3.1. Synthesis, spectroscopic data, and X-ray diffraction structures

The reaction of $Re_2(CO)_8(\mu\text{-H})(\mu\text{-}\eta^1,\eta^2\text{-CH=CHBu})$ with bma in CH_2Cl_2 proceeds slowly to produce the rhenium compounds $Re_2(CO)_8$(bma) (**2**) and $Re(CO)_4[Re(CO)_4(bma)]$ (**3**). The progress of these reactions was ascertained by TLC and IR analyses of the reaction

solution, with maximum conversion to compounds **2** and **3** being achieved in ca. two weeks time at room temperature. It is our opinion that the long reaction times required for the formation of **2** and **3** are due to the low nucleophilicity of the bma ligand. In contrast, the diphosphine ligands dppm, dppe, and (Z)-$Ph_2PCH{=}CHPPh_2$ undergo essentially quantitative substitution with **1** to give $Re_2(CO)_8$(P–P) within a few hours [17]. The direct reaction of $Re_2(CO)_{10}$ with bma in the presence of added Me_3NO was also examined as a route to compound **2**. However, the reaction of Me_3NO with the diphosphine ligand led to the decomposition of the bma ligand as evidenced by IR and TLC analyses. Compounds **2** and **3** were subsequently isolated by low-temperature column chromatography over silica gel, albeit with considerable material loss due to the silica gel-induced hydrolysis of the anhydride ring in each compound. We have encountered this behavior before during the chromatographic purification of *fac*-BrRe $(CO)_3$(bma) [5] and other bma-substituted di- and trimetal compounds [1h,3a,18].

Both **2** and **3** were characterized in solution by standard methods. The IR spectrum of $Re_2(CO)_8$(bma) in the terminal carbonyl region closely matches that of the structurally similar compound $Re_2(CO)_8$[(Z)-$Ph_2PCH{=}CHPPh_2$] and other related diphosphine-substituted derivatives [17]. The ν(CO) bands in **2** at 1830 and 1776 cm^{-1} belong to the vibrationally coupled antisymmetric and symmetric anhydride C-O stretches, respectively [19]. These frequencies found for the ν(CO) bands of the bma moiety in **2** are shifted to higher energy relative to the free ligand and are typical of other bma-substituted compounds prepared by us. A single ^{31}P resonance at $\delta - 9.37$ is consistent with equivalent phosphine groups in solution and is not unlike the chemical shift found at δ – 10.67 for phosphines in $Re_2(CO)_8$ [(Z)$Ph_2PCH{=}CHPPh_2$] [20]. The IR spectrum of $Re(CO)_4$[$Re(CO)_4$(bma)] reveals six prominent ν(CO) bands for the two $Re(CO)_4$ groups, along with bma ν(CO) bands at 1781 and 1723 cm^{-1}, whose shift to lower energy relative to **2** and free bma signifies the coordination of the bma bond to one of the $Re(CO)_4$ moieties. The chelation of the bma ligand to one of the $Re(CO)_4$ centers in **3** gives rise to the downfield ^{31}P chemical shift at δ 39.07 [21].

The photochemical and thermolysis behavior of **2** and **3** was next investigated to probe for possible C–P bond cleavage reactivity, as documented by us for bma-substituted Co_2, CoRu, and Co_3 compounds [1h,3a,18]. Both compounds are stable up to 100 °C in toluene under argon, and only begin to decompose above this temperature to unidentified non-carbonyl-containing material(s). Compound **2** is stable to near-UV irradiation at 366 nm in toluene and does not display P–C bond activation upon optical excitation unlike other bma-substituted dinuclear and polynuclear complexes prepared by our groups [3a,22]. In the case of compound **2**, these experiments allow us to rule out the possibility of $Re_2(CO)_8$(bma) serving as a precursor to $Re(CO)_4$ [$Re(CO)_4$(bma)]. No evidence for the formation of **3** from **2** was observed in any of the reactivity studies carried out. **3** undergoes slow decomposition during photolysis, as assessed by IR and TLC analyses, and was not examined any further.

Given the coordination of a $Re(CO)_4$ fragment to the bma bond in $Re(CO)_4$[$Re(CO)_4$(bma)], we investigated the reactivity of the free bond in $Re_2(CO)_8$(bma) and its potential to bind unsaturated organometallic fragments that have a known affinity for alkenes. The reactions of **2** with $Fe(CO)_4$(THF), $W(CO)_5$(THF), or $Ru_3(CO)_{12-n}(MeCN)_n$ (where $n = 1, 2$) were all unsuccessful, as judged by IR analysis. However, treatment of $Re_2(CO)_8$(bma) with $Ni(cod)_2$ in toluene at 60–70 °C led to the complete consumption of **2** within minutes. The central portion of Scheme 1 illustrates the course of this reaction. TLC analysis of the reaction solution revealed the presence of a small yellow spot ($R_f = 0.5$ in CH_2Cl_2/petroleum ether) and considerable material at the origin. Increasing the polarity of the mobile phase did not allow for the separation/observation of any other compound(s) from the origin material. The IR spectrum of the crude reaction solution exhibited an extremely broadened carbonyl pattern where the only clearly discernable frequencies were at 2086 and 1986 cm^{-1}. Chromatographic separation of the yellow spot allowed for the isolation of the phosphido-bridged complex $Re_2(CO)_8[\mu\text{-}\eta^1,\eta^1\text{-}C{=}C(PPh_2)C(O)OC(O)](\mu\text{-}PPh_2)$ in low yield. The ^{31}P NMR spectrum of **4** displays two doublet resonances ($J_{P-P} = 19.7$ Hz) at 100.01 and 10.50 that are assignable to the μ_2-PPh_2 and the PPh_2(carbocyclic ring) moieties, respectively [23].

The unequivocal identity of **2**–**4** was established by X-ray crystallography. Single crystals of each compound were found to exist as discrete molecules in the unit cell with no unusually short inter- or intramolecular contacts.

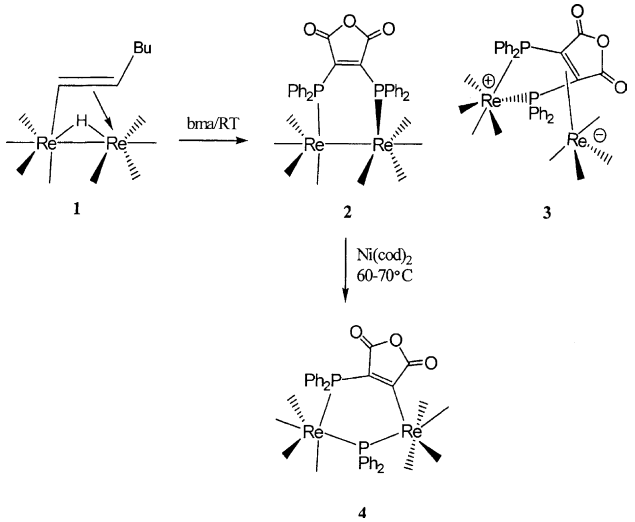

Scheme 1.

Tables 1 and 2 report the X-ray data collection and processing parameters and selected bond distances and angles, respectively.

The ORTEP diagram of $Re_2(CO)_8$(bma) shown in Fig. 1 confirms the bridging of the Re–Re vector by the bma ligand and the staggered arrangement of the equatorial groups about the Re–Re bond [24]. The Re(1)–Re(2) bond distance of 3.0593(9) Å is identical to that reported for $Re_2(CO)_{10}$ [25] and supports the presence of a Re–Re single bond that connects the two square-pyramidal $Re(CO)_4P$ groups. Coordination of the bma ligand to the $Re_2(CO)_8$ moiety leads to a minor perturbation in the planarity of the bma core as evidenced by the P(1)–C(11)–C(15)–P(2) dihedral angle of ca. 13.3. The C(11)–C(15) carbon–carbon double bond length of 1.32(2) is in good agreement with the C=C bond distance of simple alkenes and the analogous bond distance in bma- and bpcd-substituted complexes prepared by us [26]. The remaining bond distances and angles are unexceptional and do not require comment.

Fig. 2 shows the ORTEP diagram of the zwitterionic compound $Re(CO)_4[Re(CO)_4(bma)]$. Compound **3** may be conceptualized as arising from the union of the anionic, 16-electron fragment $Re(CO)_4^-$ with the cationic, 18-electron species $Re(CO)_4(bma)^+$, as facilitated by the free π bond of the bma ligand in $Re(CO)_4(bma)^+$. Each rhenium is formally six-coordinate and possesses idealized octahedral geometry, assuming that the π bond bound to Re(2) functions as a two-coordinate ligand. The nonbonded rhenium centers are electronically saturated and possess 18 valence electrons each according to the EAN rule, and the internuclear Re(1)···Re(2) bond distance of 4.76 Å exceeds the normally acceptable 2.90–3.30 Å range that is commonly found for Re–Re single bonds [27]. Coordination of the $Re(CO)_4^-$ moiety to C(11) and C(15) is accompanied by a sizeable departure from the normally observed planar environment involving the central Re(1) atom, the two phosphorus centers, and the maleic anhydride ring. In **3**, the observed torsion angles of ca. 135° and 132° for the atoms Re(1)–P(1)–C(11)–C(12) and Re(1)–P(2)–C(15)–C(14), respectively, are atypical for this diphosphine ligand and are the result of coordination of the $Re(CO)_4^-$ fragment to the C(11) and C(15) centers. The Re(1)–P(1)–C(11)–Re(2) and Re(1)–P(2)–C(15)–Re(2) torsion angles are ca. 81° and 86°, respectively. The elongation of the C(11)–C(15) bond distance to 1.56(3) Å relative to the free π bond of a bma ligand or a simple alkene is expected and in keeping with the Duncanson–Dewar–Chatt model for the bonding between an alkene and a transition metal [28]. Chelation of the bma ligand to the Re(1) center gives rise to a bond angle of 83.3(2)° for P(1)–Re(1)–P(2) atoms. The C(11)–Re(2) [2.26(2)] and C(15)–Re(2) [2.27(2) Å] bond distances and the C(11)–Re(2)–C(15) bond angle of 40.3(7)° are in agreement with distances and angles reported for several rhenium metallocyclopropane complexes [29].

The X-ray structure of $Re_2(CO)_8[\mu\text{-}\eta^1,\eta^1\text{-}\overline{C=C(PPh_2)C(O)OC(O)}](\mu\text{-}PPh_2)$, as the hexane solvate, confirms the P–C bond cleavage and loss of the Re–Re bond in $Re_2(CO)_8$(bma), as shown in the ORTEP diagram in Fig. 3. The Re(1)···Re(2) bond length of 4.36 Å precludes any direct bonding interaction between these centers. The two ReL_6 centers display idealized octahedral geometry and are tethered by a

Table 1
X-ray crystallographic data and processing parameters for the dirhenium compounds **2**–**4**

	Compound		
	2	**3**	**4**
Space group	Monoclinic, $P2_1/n$	Monoclinic, $P2_1/n$	Monoclinic, $C2/c$
a (Å)	10.1162(8)	11.888(2)	35.292(3)
b (Å)	27.928(3)	18.302(2)	10.457(1)
c (Å)	12.5221(9)	16.023(2)	20.976(2)
β (°)	95.266(6)	97.67(1)	99.944(7)
V (Å^3)	3522.8(6)	3462.6(8)	7684(1)
Molecular formula	$C_{36}H_{20}O_{11}P_2Re_2$	$C_{36}H_{20}O_{11}P_2Re_2$	$C_{39}H_{27}O_{11}P_2Re_2$
fw	1062.90	1062.90	1105.99
Formula units per cell (Z)	4	4	8
D_{calcd} (g/cm^{-3})	2.004	2.039	1.912
λ (Mo Kα) (Å)	0.71073	0.71073	0.71073
Absorption coefficient (cm^{-1})	71.08	72.3	65.21
R_{merge}	0.019	0.031	0.024
Abs corr factor	0.88–1.11	0.76–1.51	0.80–1.29
Total reflections	4705	4634	5098
Independent reflections	4421	4398	5015
Data/res/parameters	3382/0/285	2541/0/330	3163/0/356
R	0.0461	0.0439	0.0345
R_w	0.0500	0.0529	0.0381
GOF	1.34	0.71	0.61
Weights	$[0.04F^2 + (\sigma F)^2]^{-1}$	$[0.04F^2 + (\sigma F)^2]^{-1}$	$[0.04F^2 + (\sigma F)^2]^{-1}$

Table 2
Selected bond distances (Å) and angles (°) in the dirhenium compounds **2**–**4**[a]

*$Re_2(CO)_8(bma)$ (**2**) (bond distances)*			
Re(1)–Re(2)	3.0593(9)	Re(1)–P(1)	2.429(4)
Re(2)–P(2)	2.426(4)	C(11)–C(12)	1.54(2)
C(11)–C(15)	1.32(2)	C(14)–C(15)	1.55(2)
O(12)–C(12)	1.13(2)	O(13)–C(12)	1.42(2)
O(13)–C(14)	1.38(2)	O(14)–C(14)	1.16(2)
*$Re_2(CO)_8(bma)$ (**2**) (bond angles)*			
Re(2)–Re(1)–P(1)	95.1(1)	P(1)–Re(1)–C(1)	178.7(5)
Re(1)–Re(2)–P(2)	95.89(9)	P(2)–Re(2)–C(7)	177.1(5)
Re(1)–P(1)–C(11)	122.0(5)	Re(2)–P(2)–C(15)	124.0(5)
P(1)–C(11)–C(15)	132(1)	P(2)–C(15)–C(11)	133(1)
*$Re(CO)_4[Re(CO)_4(bma)]$ (**3**) (bond distances)*			
Re(1)–P(1)	2.466(5)	Re(1)–P(2)	2.473(6)
Re(2)–C(11)	2.26(2)	Re(2)–C(15)	2.27(2)
C(11)–C(15)	1.56(3)	C(11)–C(12)	1.51(2)
C(14)–C(15)	1.47(3)	O(14)–C(14)	1.20(3)
O(13)–C(14)	1.39(2)	O(13)–C(12)	1.38(2)
O(12)–C(12)	1.20(2)		
*$Re(CO)_4[Re(CO)_4(bma)]$ (**3**) (bond angles)*			
P(1)–Re(1)–P(2)	83.3(2)	C(7)–Re(2)–C(15)	154.0(8)
C(8)–Re(2)–C(11)	151.2(9)	C(11)–Re(2)–C(15)	40.3(7)
Re(1)–P(1)–C(11)	109.5(6)	Re(1)–P(2)–C(15)	109.3(7)
P(1)–Re(1)–C(3)	171.0(7)	P(2)–Re(1)–C(1)	169.1(6)
*$Re_2(CO)_8[\mu\text{-}\eta^1,\eta^2\text{-}\overline{C{=}C(PPh_2)C(O)OC}(O)](\mu\text{-}PPh_2)$ (**4**) (bond distances)*			
Re(1)–P(1)	2.497(3)	Re(1)–P(2)	2.533(3)
Re(2)–P(2)	2.513(3)	Re(2)–C(15)	2.14(1)
O(12)–C(12)	1.17(2)	O(13)–C(12)	1.37(2)
O(13)–C(14)	1.38(2)	O(14)–C(14)	1.18(2)
C(11)–C(12)	1.51(2)	C(11)–C(15)	1.35(2)
C(14)–C(15)	1.54(2)		
*$Re_2(CO)_8[\mu\text{-}\eta^1,\eta^2\text{-}\overline{C{=}C(PPh_2)C(O)OC}(O)](\mu\text{-}PPh_2)$ (**4**) (bond angles)*			
P(1)–Re(1)–P(2)	94.4(1)	P(1)–Re(1)–C(1)	178.7(4)
P(2)–Re(1)–C(2)	175.9(4)	P(2)–Re(2)–C(5)	177.2(5)
C(8)–Re(2)–C(15)	178.3(5)	Re(1)–P(1)–C(11)	120.0(4)
P(1)–C(11)–C(15)	119.9(9)	P(1)–C(11)–C(15)	129(1)
Re(2)–C(15)–C(11)	139(1)	Re(2)–C(15)–C(14)	117.7(8)

[a] Numbers in parentheses are estimated standard deviations in the least significant digits.

bridging phosphido moiety and the three-electron donor group $Ph_2P\overline{C{=}CC(O)OC}(O)$. The Re(1)–P(1) [2.497(3) Å], Re(1)–P(2) [2.533(3) Å], and Re(2)–P(2) [2.513(3) Å] bond distances fall within acceptable ranges for Re–P distances in a wide variety of rhenium compounds [30]. The internal bond angles associated with the atoms Re(1)–P(1)–C(11)–C(15)–Re(2)–P(2), that are involved in the six-membered ring that tethers the two rhenium centers, range from a low of 89.2(3)° [P(2)–Re(2)–C(15)] to a high of 139(1) [Re(2)–C(15)–C(11)]. The Re(2)–C(15) single-bond distance of 2.14(1) Å is similar to other σ-bonded rhenium compounds [31], while the C(11)–C(15) double-bond distance of 1.35(2) Å is unaffected by the activation of the bma ligand.

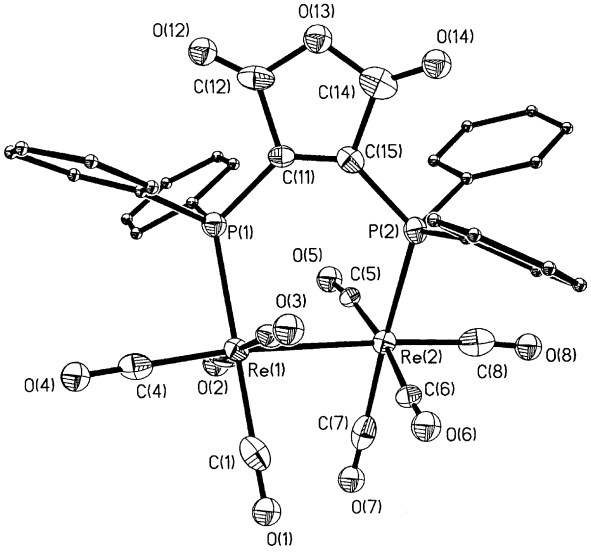

Fig. 1. ORTEP drawing of $Re_2(CO)_8(bma)$ (**2**) showing the thermal ellipsoids at the 50% probability level and phenyl carbons as spheres of arbitrary size.

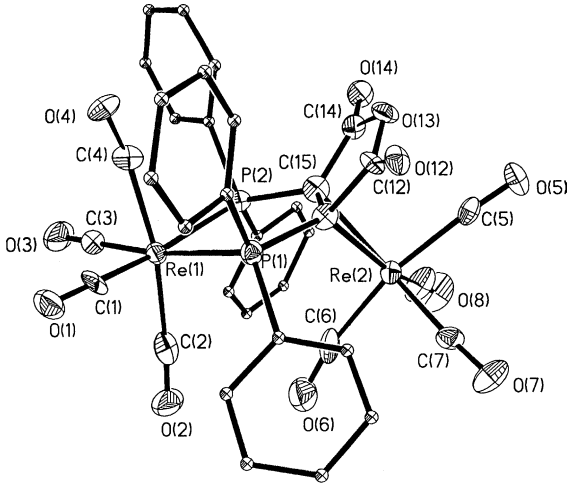

Fig. 2. ORTEP drawing of $Re(CO)_4[Re(CO)_4(bma)]$ (**3**) showing the thermal ellipsoids at the 50% probability level.

3.2. Cyclic voltammetry data and extended Hückel MO calculations

The redox properties of **2**–**4** were examined at a platinum disk electrode in CH_2Cl_2 and THF solvents containing 0.25 M TBAP as the supporting electrolyte. No major differences in the CV data as a function of the solvents were noticed. Fig. 4(a) shows the CV of $Re_2(CO)_8(bma)$ recorded at a scan rate of 0.5 V/s. Here two diffusion-controlled reductions at $E_{1/2} = -0.38$ and $E_{1/2} = -1.29$ V, ascribed to the $0/1^-$ and $1^-/2^-$ redox couples, respectively, are observed in CH_2Cl_2 solvent. Both reductions are chemically reversible given the linear plots of the current function (I_p) vs the square root of the scan rate (v) and the near unity current ratios (I_p^a/I_p^c) over the scan rates investigated [32]. The electron

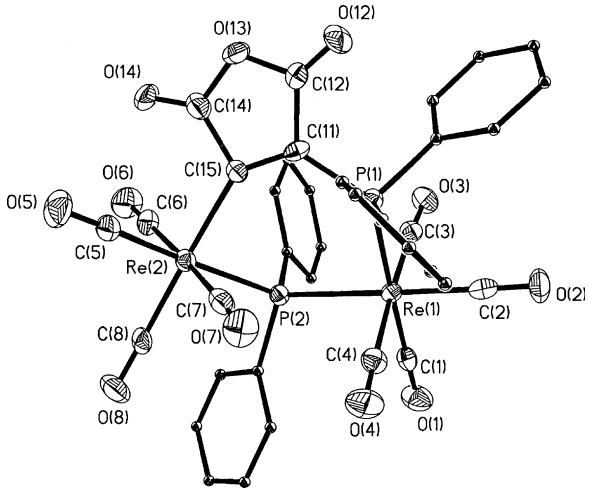

Fig. 3. ORTEP drawing of $Re_2(CO)_8[\mu\text{-}\eta^1,\eta^1\text{-}\overline{C{=}C(PPh_2)C(O)OC(O)}](\mu\text{-}PPh_2)\cdot 1/2C_6H_{14}$ (**4**) showing the thermal ellipsoids at the 50% probability level. The solvent molecule has been omitted for clarity.

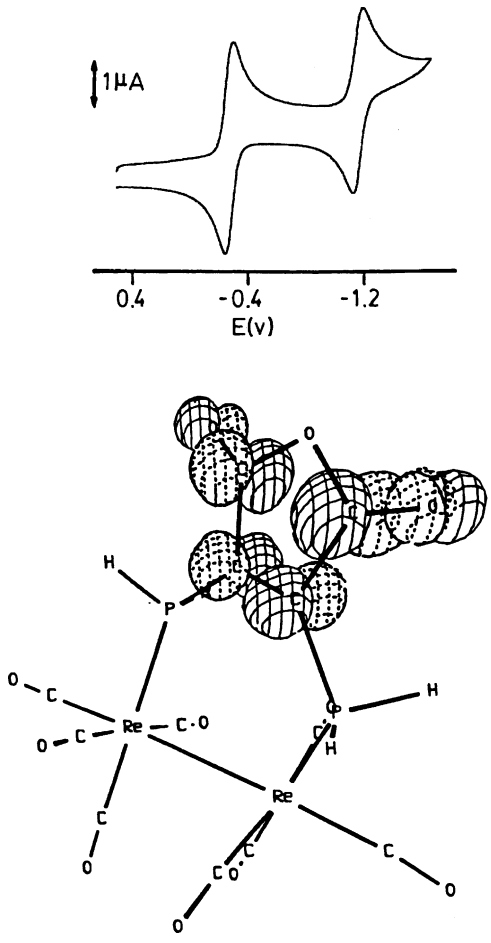

Fig. 4. Cathodic scan cyclic voltammogram for $Re_2(CO)_8$(bma) (**2**) ca. 10^{-3} M in CH_2Cl_2 containing 0.25 M TBAP at 500 mV/s at room temperature (top), and the CACAO drawing for the LUMO of $Re_2(CO)_8(H_4$-bma) (bottom).

stoichiometry was ascertained by current calibration against the known one-electron standard ferrocene [16], taking into account Walden's rule, and coulometric measurements (vide infra). The potentials found for the two reduction waves in **2** are similar to those reported by us for the mononuclear compound *fac*-BrRe(CO)$_3$(bma) [5], and these data are not surprising given the commonality of the LUMO in bma-ligated complexes. An irreversible oxidation at $E_p^a = 1.09$ V ($v = 0.1$ V/s) was also observed when the sample is scanned out to 1.5 V. Increasing the scan rate to 1.0 V/s (room temperature) or lowering the temperature to −60 °C ($v = 0.1$ V/s) increased the I_p^c/I_p^a ratio to 0.55 and 0.75, respectively.

$Re_2(CO)_8$(bma) was further investigated by constant-potential coulometry (CPC) in order to gain more information concerning the nature of $[Re_2(CO)_8(bma)]^{\cdot -}$ and site of electron accession. $Re_2(CO)_8$(bma) was reduced at room temperature in THF at −0.75 V, and the total charge passed upon completion of reduction was calculated to $Q = 0.95$ C/mol of $Re_2(CO)_8$(bma). The magnitude of Q obtained by the CPC experiment is in excellent agreement with the one-electron stoichiometry determined by using CV criteria [32]. The catholyte was analyzed by IR spectroscopy so that the effect of the added electron on the carbonyl bands could be explored. $[Re_2(CO)_8(bma)]^{\cdot -}$ exhibits ν(CO) bands at 2064 (s), 2009 (s), 1969 (vs), 1944 (m), 1937 (m), 1908 (s), 1739 (w), and 1656 (s) cm^{-1}. The carbonyl bands belonging to the $Re_2(CO)_8$ moiety in the radical anion have shifted from 11 to 20 cm^{-1} to lower energy relative to the neutral starting material [33]. The magnitude of these frequency shifts indicates that little of the added electron density in $[Re_2(CO)_8(bma)]^{\cdot -}$ resides on the rhenium centers and the terminal carbonyl groups. The predominant locus associated with the reduction is the bma ligand as revealed by the dramatic shift in the carbonyl bands of the anhydride residue. Here the ν(CO) bands of the reduced ligand have shifted 91 and 120 cm^{-1} to lower energy relative the ν(CO) bands at 1830 and 1776 cm^{-1} for $Re_2(CO)_8$(bma) and are entirely consistent with the reports on sundry other $18 + \delta$ compounds characterized to date [1,2,5]. Corroboration of the electron stoichiometry and the site of reduction was also demonstrated by parallel experiments conducted with the known one-electron reducing agent Cp_2Co. Treatment of $[Re_2(CO)_8(bma)]$ with cobaltocene (1.0 mol equiv) in THF at room temperature lead to the immediate formation of $[Re_2(CO)_8(bma)]^{\cdot -}$ in quantitative yield as determined by IR spectroscopy. The IR spectrum of $[Re_2(CO)_8(bma)][Cp_2Co]$ was identical to that obtained by bulk electrolytic reduction, removing any ambiguity as to the identity of the radical anion. Finally, we attempted to grow single crystals of $[Re_2(CO)_8$-(bma)$][Cp_2Co]$ for X-ray diffraction analysis but not were successful and abandoned that avenue for the characterization of the radical anion.

The redox chemistry of compounds **3** and **4** was briefly examined by CV. $Re(CO)_4[Re(CO)_4(bma)]$ exhibits an irreversible reduction at $E_p^c = -1.85$ V in THF containing 0.1 M TBAP at a scan rate of 0.5 V/s, with anodic peaks detected at $E_p^a = -1.20$ V and $E_p^a = -0.52$ V on the return scan. Increasing the scan rate up to 5.0 V/s did not improve the irreversible behavior of the reduction wave in $Re(CO)_4[Re(CO)_4(bma)]$. The phosphido-bridged complex $Re_2(CO)_8[\mu\text{-}\eta^1,\eta^1\text{-}\overline{C{=}C(PPh_2)C(O)OC(O)}](\mu\text{-}PPh_2)$ displays a single reduction at $E_{1/2} = -1.21$ V in CH_2Cl_2 in 0.25 M TBAP. The peak-to-peak separation of 124 mV is slightly larger than that found for internally added ferrocene, whose ΔE_p was 75 mV, and suggests a slow electron transfer (i.e., k_{het} low) for this redox couple.

The orbital composition of the HOMO and LUMO levels in the model complexes $Re_2(CO)_8(H_4\text{-bma})$, $Re(\underline{CO)_4[Re(CO)_4(H_4}\text{-bma})]$, and $Re_2(CO)_8[\mu\text{-}\eta^1,\eta^1\text{-}\overline{C{=}C(PH_2)C(O)OC(O)}](\mu\text{-}PH_2)$ was examined by extended Hückel MO calculations in an effort to understand more fully the observed electrochemistry in compounds **2**–**4**. The HOMO in $Re_2(CO)_8(H_4\text{-bma})$, which occurs at −11.82 eV, is composed of an in-phase overlap of d_z^2 orbitals on the rhenium centers that follows the general bonding pattern typified by the interaction of two $d^7\text{-}ML_5$ fragments [28,34]. The LUMO in $Re_2(CO)_8(H_4\text{-bma})$ exhibits an orbital energy of −9.98 eV and is located exclusively on the maleic anhydride residue. Fig. 4(b) shows the CACAO diagram [14] of the LUMO in $Re_2(CO)_8(H_4\text{-bma})$. The antibonding π^* character displayed by the LUMO $Re_2(CO)_8(H_4\text{-bma})$ is akin to that of ψ_4 found in simple six-π-electron systems like maleic anhydride and 1,3,5-hexatriene, and the related compound *fac*-$BrRe(CO)_3(H_4\text{-bma})$ [5]. The π^* character of the LUMO in $Re_2(CO)_8(H_4\text{-bma})$ explains fully the reductive electrochemistry that is largely localized on the bma ligand in $Re_2(CO)_8(bma)$ and is in keeping with the redox chemistry reported for a wide variety of bma-substituted complexes [1a–1f,2,5,22].

The HOMO and LUMO levels in the zwitterionic compound $Re(CO)_4[Re(CO)_4(H_4\text{-bma})]$ may be viewed as arising from the union of the anionic $d^8\text{-}ML_4$ species $Re(CO)_4^-$ and the octahedral cation $Re(CO)_4(H_4\text{-bma})^+$, as depicted below. The empty π^* acceptor orbital on $Re(CO)_4(H_4\text{-bma})^+$ corresponds to the ϕ_4 MO associated with the bma moiety, as discussed above for $Re_2(CO)_8(H_4\text{-bma})$. This empty bma orbital has the correct symmetry for strong overlap with its filled b_2 counterpart on the $Re(CO)_4^-$ fragment, whose nodal properties are well known and mimic that of its isolobal cousin CH_2 [35]. In-phase and out-of-phase overlap of the bma-acceptor orbital with the d_{xz} hybrid orbital on the $Re(CO)_4^-$ fragment leads to the HOMO (−11.94 eV) and the LUMO (−9.32 eV), respectively, as shown by the CACAO drawings in Fig. 5. The HOMO and LUMO both contain essentially equal contributions from the maleic anhydride moiety and rhenium metal character from the π-bound $Re(CO)_4^-$ fragment. On the basis of these data, electron addition to this LUMO by either electrochemical or chemical methods is expected to furnish a very unstable radical anion, whose pathway for decomposition could well involve the loss of the 16-electron species $Re(CO)_4^-$ and the neutral radical $[Re(CO)_4(H_4\text{-bma})]^{\cdot}$. Independent experiments designed to test this premise are planned for the future.

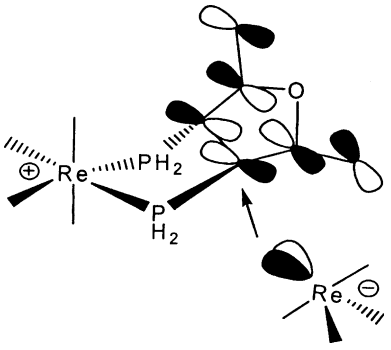

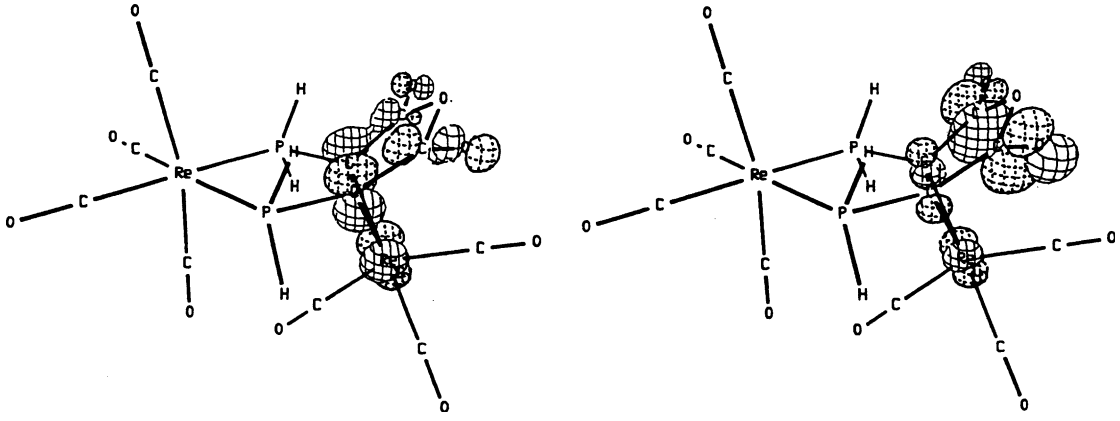

Fig. 5. CACAO drawings for the HOMO (left) and the LUMO (right) of $Re(CO)_4[Re(CO)_4(H_4\text{-bma})]$.

The HOMO in $Re_2(CO)_8[\mu\text{-}\eta^1,\eta^1\text{-}\overline{C{=}C(PH_2)C(O)OC}\text{-}(O)](\mu\text{-}PH_2)$ consists of contributions from both metals in the form of hybridized d_{yz} orbitals and the π bond of the maleic anhydride ring, as shown below. The HOMO occurs at −12.49 eV and clearly exhibits an in-phase dπ–pπ bonding interaction involving the maleic anhydride carbon atom that is sigma-bound to the rhenium center in compound **4**. The LUMO, which occurs at −10.14 eV, is a maleic anhydride-based orbital whose nodal symmetry approximates that of *rpsi*$_4$, as previously discussed for $Re_2(CO)_8(H_4\text{-bma})$. Completing the overall picture in the LUMO is a minor antibonding interaction present between the π^* system of the anhydride ring and the sigma-bound Re center.

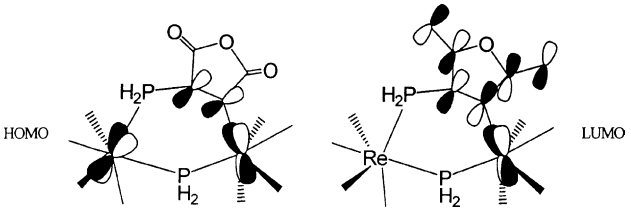

4. Conclusions

The diphosphine ligand bma reacts with $Re_2(CO)_8(\mu\text{-}H)(\mu\text{-}\eta^1,\eta^2\text{-}CH{=}CHBu)$ to give the expected product of substitution $Re_2(CO)_8(bma)$ and the zwitterionic compound $Re(CO)_4[Re(CO)_4(bma)]$. The structural composition of this latter compound has not been observed previously in reactions between the alkenyl complexes $Re_2(CO)_8(\mu\text{-}H)(\mu\text{-}\eta^1,\eta^2\text{-alkenyl})$ and unsaturated diphosphine ligands. Both of these dirhenium compounds are relatively stable, but in the case of $Re_2(CO)_8(bma)$ thermolysis with added $Ni(cod)_2$ affords the phosphido-bridged compound $Re_2(CO)_8[\mu\text{-}\eta^1,\eta^1\text{-}\overline{C{=}C(PPh_2)C(O)OC(O)}](\mu\text{-}PPh_2)$.

5. Supporting information available

Crystallographic data for the structural analyses have been deposited with the Cambridge Crystallographic Data Center, CCDC no. 220768 for **2**; 220769 for **3**; 220770 for **4**. Copies of this information may be obtained free of charge from the Director, CCDC, 12 Union Road, Cambridge, CB2 1EZ UK [Fax: +44(1223)336-033; email: deposit@ccdc.ac.uk or http://www.ccdc.cam.ac.uk.

Acknowledgements

Financial support from the Robert A. Welch Foundation (B-1093-MGR) is appreciated. We also thank the Cyprus Sierrita Corporation for their generous gift of ammonium perrhenate.

References

[1] (a) D. Fenske, H.J. Becher, Chem. Ber. 107 (1974) 117;
Chem. Ber. 108 (1975) 2115;
(b) D. Fenske, Chem. Ber. 112 (1979) 363;
(c) W. Bensmann, D. Fenske, Angew. Chem. Int. Ed. Engl. 17 (1978) 462;
(d) D. Fenske, A. Christidis, Angew. Chem., Int. Ed. Engl. 20 (1981) 129;
(e) D.R. Tyler, Acc. Chem. Res. 24 (1991) 325;
(f) M. Fei, S.K. Sur, D.R. Tyler, Organometallics 10 (1991) 419;
(g) N.W. Duffy, R.R. Nelson, M.G. Richmond, A.L. Rieger, P.H. Rieger, B.H. Robinson, D.R. Tyler, J.C. Wang, K. Yang, Inorg. Chem. 37 (1998) 4849;
(h) S.G. Bott, K. Yang, J.C. Wang, M.G. Richmond, Inorg. Chem. 39 (2000) 6051.
[2] (a) F. Mao, D.R. Tyler, D. Keszler, J. Am. Chem. Soc. 111 (1989) 130;
(b) F. Mao, D.R. Tyler, M.R.M. Bruce, A.E. Bruce, A.L. Rieger, P.H. Rieger, J. Am. Chem. Soc. 114 (1992) 6418;
(c) D.M. Schut, K.J. Keana, D.R. Tyler, P.H. Rieger, J. Am. Chem. Soc. 117 (1995) 8939.
[3] (a) K. Yang, J.M. Smith, S.G. Bott, M.G. Richmond, Organometallics 12 (1993) 4779;
(b)See also: S.G. Bott, H. Shen, M.G. Richmond, Struct. Chem. 12 (2001) 225.
[4] (a) C.-G. Xia, S.G. Bott, M.G. Richmond, Organometallics 15 (1996) 4480;
(b) S.G. Bott, K. Yang, M.G. Richmond, Organometallics 22 (2003) 1383;
(c) S.G. Bott, H. Shen, R.A. Senter, M.G. Richmond, Organometallics 22 (2003) 1953.
[5] K. Yang, S.G. Bott, M.G. Richmond, Organometallics 14 (1995) 2387.
[6] (a)For two other related rhenium structures bearing redox-active diphosphine ligands, see: C.-G. Xia, S.G. Bott, M.G. Richmond, Inorg. Chim. Acta 230 (1995) 45;
(b) K. Yang, S.G. Bott, M.G. Richmond, J. Chem. Crystallogr. 33 (2003).
[7] F. Mao, C.E. Philbin, T.J.R. Weakley, D.R. Tyler, Organometallics 9 (1990) 1510.
[8] A. Roedig, L. Hörnig, Chem. Ber. 88 (1955) 2003.
[9] L.S. Crocker, G.L. Gould, D.M. Heinekey, J. Organomet. Chem. 342 (1988) 243.
[10] P.O. Nubel, T.L. Brown, J. Am. Chem. Soc. 104 (1982) 4955;
J. Am. Chem. Soc. 106 (1984) 644.
[11] R.B. King, in: Organometallic Syntheses, vol. 1, Academic Press, New York, 1965.
[12] D.F. Shriver, The Manipulation of Air-Sensitive Compounds, McGraw-Hill, New York, 1969.
[13] (a) R. Hoffmann, W.N. Lipscomb, J. Chem. Phys. 36 (1962) 2179;
(b) R. Hoffmann, J. Chem. Phys. 39 (1963) 1397.
[14] C. Mealli, D.M. Proserpio, J. Chem. Ed. 67 (1990) 399.
[15] R.C. Weast (Ed.), Handbook of Chemistry and Physics, 56th ed, CRC Press, Cleveland, OH, 1975.
[16] A.J. Bard, L.R. Faulkner, Electrochemical Methods, Wiley, New York, 1980.
[17] (a) K.-W. Lee, W.T. Pennington, A.W. Cordes, T.L. Brown, Organometallics 3 (1984) 404;
(b) S.G. Bott, K. Yang, M.G. Richmond, J. Chem. Crystallogr. 31 (2001) 485.

[18] (a) K. Yang, S.G. Bott, M.G. Richmond, Organometallics 13 (1994) 3788;
(b) H. Shen, S.G. Bott, M.G. Richmond, Inorg. Chim. Acta 250 (1996) 195.
[19] D. Dolphin, A. Wick, Tabulation of Infrared Spectral Data, Wiley-Interscience, New York, 1977.
[20] Unpublished results.
[21] (a) P.E. Garrou, Chem. Rev. 81 (1981) 229;
(b) M.G. Richmond, J.K. Kochi, Organometallics 6 (1987) 254.
[22] K. Yang, J.A. Martin, S.G. Bott, M.G. Richmond, Organometallics 15 (1996) 2227.
[23] (a) A.J. Carty, S.A. MacLaughlin, D. Nucciarone, in: J.G. Verkade, L.D. Quin (Eds.), Phosphorus-31 NMR Spectroscopy in Stereochemical Analysis: Organic Compounds and Metal Complexes, VCH Publishers, New York, 1987 (Chapter 16);
(b) A.J. Carty, Adv. Chem. Ser. 192 (1982) 163.
[24] A.E. Leins, D.G. Billing, D.C. Levendis, J. du Toit, N.J. Coville, Inorg. Chem. 31 (1992) 4756.
[25] M.R. Churchill, K.N. Amoh, H.J. Wasserman, Inorg. Chem. 20 (1981) 1609.
[26] (a) K. Yang, S.G. Bott, M.G. Richmond, J. Organomet. Chem. 516 (1996) 65;
(b) S.G. Bott, H. Shen, M.G. Richmond, J. Chem. Crystallogr. 28 (1998) 385;
(c) S.G. Bott, J.C. Wang, H. Shen, M.G. Richmond, J. Chem. Crystallogr. 29 (1999) 391;
(d) S.G. Bott, H. Shen, M.G. Richmond, Struct. Chem. 12 (2001) 237.
[27] B.F.G. Johnson, in: B.F.G. Johnson (Ed.), Transition Metal Clusters, Wiley, New York, 1980 (Chapter 1).
[28] T.A. Albright, J.K. Burdett, M.H. Whangbo, Orbital Interactions in Chemistry, Wiley, New York, 1985.
[29] (a) R.D. Adams, G. Chen, J. Yin, Organometallics 10 (1991) 1278;
(b) C.P. Casey, Y. Ha, D.R. Powell, J. Organomet. Chem. 472 (1994) 185;
(c) C.P. Casey, R.S. Cariño, R.K. Hayashi, K.D. Schladetzky, J. Am. Chem. Soc. 118 (1996) 1617.
[30] A.G. Orpen, L. Brammer, F.H. Allen, O. Kennard, D.G. Watson, R. Taylor, J. Chem. Soc., Dalton Trans. (1989) S1.
[31] (a) R.D. Adams, M. Huang, Organometallics 15 (1996) 4437;
(b) B.M. Handwerker, K.E. Garrett, K.L. Nagle, G.L. Geoffroy, A.L. Rheingold, Organometallics 9 (1990) 1562.
[32] (a)For the normal criteria associated with CV reversibility, see: R.N. Adams, Electrochemistry at Solid Electrodes, Marcel Dekker, New York, 1969;
(b) P.H. Rieger, Electrochemistry, Chapman & Hall, New York, 1994;
(c)See also Ref. [16].
[33] Cf. the IR data in THF for $Re_2(CO)_8$ (bma) where ν(CO) bands are found at 2075 (s), 2023 (s), 1983 (vs), 1957 (m), 1950 (m, sh), 1927 (s), 1830 (vw, antisymm anhydride carbonyl), 1776 (s, symm anhydride carbonyl) cm^{-1}.
[34] S. Shaik, R. Hoffmann, C.R. Fisel, R.H. Summerville, J. Am. Chem. Soc. 102 (1980) 4555.
[35] (a)For a few reports on the bonding between ML_4 fragments and alkenes, see T.A. Albright, R. Hoffmann, J.C. Thibeault, D.L. Thorn, J. Am. Chem. Soc. 101 (1979) 3801;
(b) T.A. Albright, R. Hoffmann, Y.-C. Tse, T. D'Ottavio, J. Am. Chem. Soc. 101 (1979) 3812;
(c) O. Eisenstein, R. Hoffmann, J. Am. Chem. Soc. 103 (1981) 4308;
(d) T.A. Albright, Acc. Chem. Res. 15 (1982) 149.